

Explore and Match: End-to-End Video Grounding with Transformer

Sangmin Woo, Jinyoung Park, Inyong Koo, Sumin Lee, Minki Jeong, Changick Kim

Korea Advanced Institute of Science and Technology (KAIST)

{smwoo95, jinyoungpark, iykoo010, suminlee94, rhm033, changick}@kaist.ac.kr

Abstract

We present a new paradigm named *explore-and-match* for video grounding, which aims to seamlessly unify two streams of video grounding methods: *proposal-based* and *proposal-free*. To achieve this goal, we formulate video grounding as a set prediction problem and design an end-to-end trainable Video Grounding Transformer (VIDGTR) that can utilize the architectural strengths of rich contextualization and parallel decoding for set prediction. The overall training is balanced by two key losses that play different roles, namely *span localization loss* and *set guidance loss*. These two losses force each proposal to regress the target timespan and identify the target query. Throughout the training, VIDGTR first explores the search space to diversify the initial proposals, and then matches the proposals to the corresponding targets to fit them in a fine-grained manner. The *explore-and-match* scheme successfully combines the strengths of two complementary methods, without encoding prior knowledge into the pipeline. As a result, VIDGTR sets new state-of-the-art results on two video grounding benchmarks with double the inference speed.

1. Introduction

The explosion of video data brought on by the growth of the internet poses challenges to effective video search. In order to accomplish successful video search, much effort has been put into language query-based video retrieval [9, 12, 30, 48, 49]. While text-video retrieval aims to match a trimmed video clip to the language query, video grounding aims to find accurate timespans relevant to the language queries in an untrimmed video. It can be helpful especially when one wants to find a specific scene in a long video, such as a movie. The majority of existing methods for video grounding can be categorized into two families: 1) *proposal-based* methods [2, 5, 13, 14, 17, 25, 26, 33, 43, 45, 48, 50, 54, 56, 57, 58], which

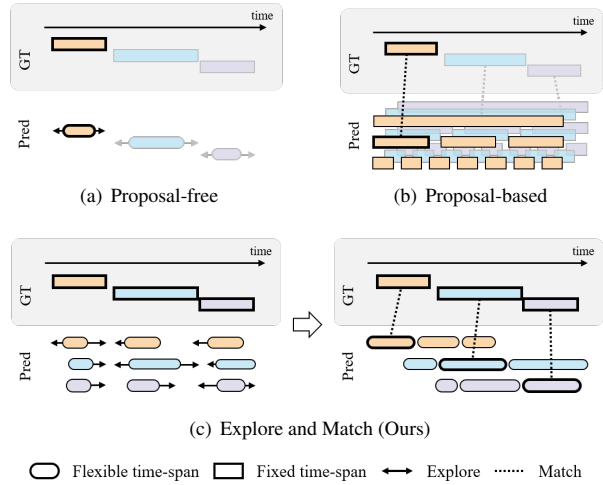


Figure 1. (a) **Proposal-free** methods directly regress start and end timestamps. (b) **Proposal-based** methods exhaustively match all predefined fixed-size proposals with ground truths. (c) Our **explore-and-match** paradigm unifies two methods, eliminating the hand-crafted proposals, and instead makes flexible timespan proposals. Unlike previous methods that predict one sentence in a single loop, our approach predicts multiple sentences at once.

generate a bunch of proposals in advance and select the best match with target spans, and 2) *proposal-free* methods [6, 7, 8, 15, 29, 31, 36, 42, 45, 52, 53, 55], which estimate start and end timestamps aligned to the given description directly. The *proposal-based* approaches generally show strong performance at the expense of prohibitive cost of proposal generation. They contradict the end-to-end philosophy, and their performances are significantly influenced by hand-designed pre- or post-processing steps such as dense proposal generation [10, 47] or non-maximum suppression [39, 45, 51] to abandon near-duplicate predictions. On the other hand, the *proposal-free* approaches are much more efficient, but involve difficulties in optimization since the search space for final timespan prediction is too large.

In this work, we present a new video grounding paradigm named **explore-and-match**, which integrates the strengths of the two aforementioned approaches by formulating video grounding as a direct set prediction problem.

All codes and models will be made available shortly.

Our method keeps the use of proposals while flexibly predicting timespans. Also, it eliminates time-consuming pre- and post-processing via a direct set prediction. A conceptual comparison of our approach with two approaches is shown in Fig. 1. To solve video grounding as a set prediction problem, we introduce an end-to-end trainable model called VIDGTR based on the transformer encoder-decoder architecture [41]. The primary ingredients of VIDGTR are bipartite set matching and parallel decoding with a small set of learnable proposals. We refer to trainable positional encodings as *learnable proposals* that are transformed in parallel into timespans by the transformer decoder. To train all learnable proposals in parallel, we adopt the Hungarian algorithm [21] to find the optimal bipartite matching (*i.e.*, paired in a way that minimizes the matching cost) between ground truths and predictions. This guarantees that each target has a unique match during training. The self-attention mechanism of the transformer enables all elements in an input sequence to interact with one another, making transformer architecture particularly suitable for certain constraints of set prediction, such as suppressing duplicate predictions. By design, VIDGTR allows us to forgo the use of manually-designed components (*e.g.*, temporal anchors, windows) that encode prior knowledge into the video grounding pipelines. Furthermore, learnable proposals can interact with visual-linguistic representations as well as themselves to directly output the final timespan predictions in a single pass.

In our **explore-and-match** scheme, all learnable proposals diversify while **exploring** span space, and subsequently **match** their corresponding targets. However, the model becomes unable to associate each prediction with an individual target since the transformer architecture does not encode positional information of the input sequence (*i.e.*, target-agnostic). The overall training is governed by bipartite set matching with span localization loss and set guidance loss. The span localization loss leads proposals to generate precise timespans. On the other hand, set guidance loss makes VIDGTR generate the target-specific predictions. We generate subgroups by dividing the learnable proposals by the number of sentences. Then, our set guidance loss gradually force each subset of proposals to predict the input order of the corresponding language query. At the beginning of training, each ground truth is assigned with a random proposal since set matching is largely driven by the span localization loss. Once the timespan proposals align with ground truths in a target-agnostic manner, the set guidance loss becomes dominant, and learnable proposals begin to predict the timespan of the designated target. Finally, the learnable proposals are fit to their respective target spans. The overall prediction-target matching is trained in a set-to-set manner. While the strategy conforms to the end-to-end basis, it spontaneously divides and conquers the entire process in-

stead of optimizing all the objectives as a whole. Under the explore-and-match scheme, VIDGTR starts by generating diverse initial timespan proposals that are target-agnostic, which are then regressed to match the specific target accurately. With set-to-set matching, the proposals in different subsets can peek at each other and cooperatively build an optimal set of timespans. We show the empirical evidence of the explore-and-match phenomenon and confirm that this simple strategy is remarkably effective.

We evaluate VIDGTR trained under explore-and-match regime on two challenging video grounding benchmarks — *ActivityCaptions* [3, 20] and *Chrades-STA* [13] — against the recent works. Our VIDGTR achieves new state-of-the-art results on two benchmarks, even without human priors such as knowledge of timespan distribution. In addition, we conduct extensive ablation studies and analyses on our method. To summarize, our contributions are three-fold:

- We introduce a new video grounding paradigm, “explore-and-match”, which unifies the strengths of *proposal-based* and *proposal-free* methods.
- We propose an end-to-end trainable model, VIDGTR, which models the video grounding as a set prediction problem. This formulation streamlines the overall pipeline by removing the use of several heuristics.
- Comprehensive experiments and extensive ablation studies demonstrate the effectiveness of VIDGTR. Moreover, VIDGTR sets a new state-of-the-art on two video grounding benchmarks while being two times faster than previous methods.

2. Related Work

Video Grounding. The origin of video grounding traces back to the temporal activity localization [37], which attempts to locate the start and end timestamps of actions and identify its labels in an untrimmed video. Likewise, video grounding aims to retrieve the corresponding timespans, but it is grounded on language queries rather than a fixed set of action labels. Pioneering video grounding works [2, 13] define the task and provide benchmark datasets. Since then, numerous efforts have been made to push the boundaries of video grounding. Early works follow the *proposal-based* pipeline [2, 5, 13, 14, 17, 25, 26, 33, 43, 45, 48, 50, 54, 56, 57, 58], which segments a huge number of candidate timespans at regular intervals on different scales, and then ranks them using an evaluation network. While *proposal-based* approaches show reliable results, they are sensitive to proposal quality and suffer from the prohibitive cost of creating proposals, as well as the computationally inefficient comparison of all proposal-target pairings. Another line of works are the *proposal-free* approaches [6, 7, 8, 15, 29, 31, 36, 42, 45, 52, 53, 55], which tries to regress the timespans directly. They are more flexible than *proposal-based* approaches in terms of granularity.

However, its accuracy generally lags behind that of its counterpart. To summarize, the former try to **match** the predefined proposals with ground truth, while the latter **explore** the whole search space to find timespans directly.

In this work, we aim to integrate two streams of video grounding methods into a single paradigm named explore-and-match, by formulating video grounding as a direct set prediction problem. Our method can generate flexible timespans like *proposal-free* approaches while preserving the concept of *proposal-based* approaches that use positive and negative proposals at the same time.

Transformers. A transformer [41] is an universal sequence processor with an attention-based encoder-decoder architecture. The self-attention mechanism captures both long-range interactions in a single context, and the encoder-decoder attention takes into account of token correspondences across multi modalities. Due to the tremendous promise of the attention mechanism, transformers have recently demonstrated their potential in various computer vision tasks: object detection [4], video instance segmentation [46], panoptic segmentation [44], human pose and mesh reconstruction [23], lane shape prediction [27], and human object interaction [59].

Among these, it is worth noting that the Detection Transformer (DETR) [4], the first transformer-based end-to-end object detector, achieved very competitive performance despite its simple design. DETR successfully removes many hand-crafted components in the object detection pipeline by exploiting the powerful relation modeling capability of transformers. The principal loss of DETR is based on bipartite matching, notably the Hungarian algorithm [21], which generates a set of unique bounding boxes. This saves a lot of post-processing time by removing non-maximum suppression from the pipeline. Also, DETR infers a set of predictions in parallel with a single iteration through the decoder.

Inspired by the recent successes of transformers, we propose a novel video grounding model named VIDGTR based on the transformer architecture. The attention mechanism of transformer allows every element of the input sequence to attend to each other while utilizing rich contextualization. This architectural strength makes transformer particularly suitable for our video grounding formulation, a direct set matching problem. We note that final timespan predictions are directly generated in an end-to-end manner.

3. Method

We first define the video grounding task, and propose our end-to-end trainable VIDGTR. Next, we introduce our training losses and set matching scheme. Finally, we present explore-and-match, a new paradigm that unifies *proposal-based* and *proposal-free* methods.

3.1. Problem Formulation

Video grounding aims to localize a set of language-grounded timespans in an untrimmed video. Since video grounding does not have a fixed set of sentence classes, the conventional classification approach is not applicable (*i.e.*, taxonomy-free). Therefore, the video grounding model should be able to infer the timespans while not being constrained by the predefined categories. Formally, given a video \mathcal{V} with a set of language queries $\mathcal{Q} = \{q_i\}_{i=1}^K$, we require a set of corresponding timespans.

$$\{y_i\}_{i=1}^K = \{(t_i, q_i)\}_{i=1}^K, \quad (1)$$

where $t_i = (t_i^s, t_i^e) \in [0, 1]$ defines start and end timestamp normalized by the video length, and K is the number of the queries. If $K = 1$, the model only expects a single sentence as an input query, which is a conventional single-query setting. In this setting, there is no need for prediction-query assignment since all the predictions of learnable proposals can be associated with only one target (*i.e.*, q_i can be omitted in (1)). However, this limits the abundant interactions of the transformer with parallel decoding. In order to account for beneficial semantic and temporal relationships between the timespans, we view video grounding as a direct set prediction problem. In a multi-query setting, the model needs to specify which predictions are paired with which queries. Therefore, the grounding model should assign correct queries to the estimated timespans:

$$\{\hat{y}_i\}_{i=1}^N = \{(\hat{t}_i, \hat{q}_i)\}_{i=1}^N, \quad (2)$$

where \hat{t} and \hat{q} denote the predicted timespans and queries, respectively. The number of predictions N is substantially larger than the actual number of queries K in the video.

3.2. VidGTR Architecture

The overall pipeline of VIDGTR is illustrated in Fig. 2. VIDGTR contains three main components: 1) a feature extractor to obtain a compact video and text representations, 2) a transformer encoder-decoder for contextualization and parallel decoding, and 3) a feed-forward network (FFN) that makes the final span predictions.

Feature Extractor. An input video $\mathcal{V} \in \mathbb{R}^{T_0 \times C_0 \times H_0 \times W_0}$ passes through the C3D [40] (typical values we use are $T_0 = 16$, $C_0 = 3$ and $H_0 = W_0 = 112$), and is transformed into a video feature $f_v \in \mathbb{R}^{T \times C \times H \times W}$ ($T = 1$, $C = 512$ and $H = W = 4$). Since the input to transformer encoder should be in the form of sequence, we collapse the channel and spatial dimensions into a single dimension ($T \times CHW$). Then, we feed the output into a linear layer, which yields $T \times D$ dimensions. On the other hand, input language queries \mathcal{Q} break down into a set of word sequences, and then are converted into GloVe [32] embeddings. A set of sentence representations $f_t \in \mathbb{R}^{K \times D}$ ($K \geq 1$, $D = 512$) is obtained via a 2-layer bi-LSTM [18], followed by a linear

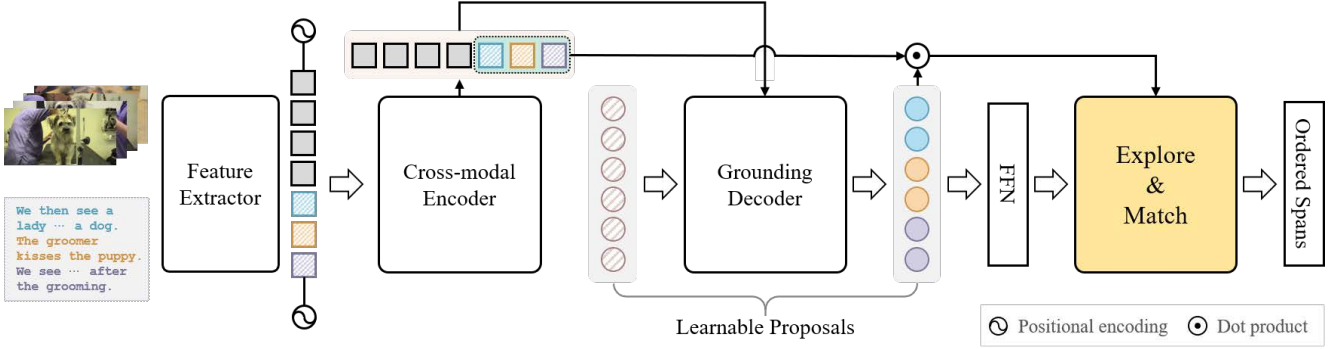


Figure 2. From the **feature extractor**, we first obtain video and text features and supplement them with positional encoding. The **encoder** takes as input a sequence of concatenated video-text features. The **decoder** is fed with a fixed number of *learnable proposals*, which in turn attend to themselves and the encoder output, generating contextualized outputs. These outputs are then used to predict the timespans via a **prediction head** (i.e., FFN) and measure the correspondence with the textual outputs of the encoder using a dot product (\odot). Hereafter, the overall training process follow the *explore-and-match* scheme (See more details in Fig. 3). VIDGTR directly generates a set of ordered timespans in parallel, and the training is done in an end-to-end manner.

layer. The input sentences are batch-processed by applying zero-padding to have the same dimension K as the largest number of sentences within the batch. For a fair comparison, VIDGTR is equipped with a conventional C3D+LSTM backbone, but it can be trained on top of any modern backbone (e.g., CLIP [34], ViT [11]).

Video Grounding Transformer. The video features and text features obtained from the feature extractor. We concatenate video-text features and pass into the transformer encoder. The transformer¹ is unable to preserve the order of temporally arranged video features due to the permutation-invariant nature of the architecture. Therefore, we add fixed positional encodings to concatenated video-text features at every attention layer. Each encoder layer has two sub-layers: a multi-head self-attention layer and a feed-forward network. The key component of the encoder is self-attention, which relates different positions of a single sequence to compute an intra-representation of the sequence. The decoder structure adds encoder-decoder attention in addition to the two sub-layers in the encoder. The decoder takes a fixed-size set of N inputs, which we refer to as *learnable proposals*, and decodes them into a set of N output embeddings. All proposals collaboratively generate predictions in a set-wise manner with self-attention while being able to access the whole video-text context with encoder-decoder attention. The output embeddings from the decoder are fed into the prediction head, resulting in N final timespan predictions. The prediction head is a 2-layer perceptron with a two-dimensional output, which is set to predict start and end timestamps. To match the proposals to corresponding sentences, we measure their correspondence with normalized similarity of the decoder output and textual output of the encoder. This is used to link each prediction to the query with the highest similarity.

¹The architectural details of the transformer are elaborated in the supplementary material.

3.3. Explore and Match

Considering that video includes multiple events over various time periods, we define video grounding as a set prediction problem. To solve a set prediction problem between predicted and ground truth spans, we adopt a Hungarian matching algorithm [21]. Based on the matching results, we define our final set prediction loss. Finally, we present a new training paradigm named *explore-and-match*. We then elaborate on how it can combine two streams of methods, *proposal-based* and *proposal-free*.

Video grounding as a set prediction. We search for one-to-one matching between the prediction set $\{\hat{y}_i\}_{i=1}^N$ and the ground truth set $\{y_i\}_{i=1}^K$ that optimally assigns predicted timespans to each ground truth. We assume that the number of predictions N is sufficiently larger than the number of queries K in the video. Therefore, we consider the ground truth set y as a set of size N padded with \emptyset (no matching) for one-to-one matching. We define a set of all permutations that consist of N items as \mathfrak{S}_N . Among the set of permutations \mathfrak{S}_N , we seek an optimal permutation $\hat{\sigma} \in \mathfrak{S}_N$ that best assigns the predictions at the lowest cost:

$$\hat{\sigma} = \operatorname{argmin}_{\sigma \in \mathfrak{S}_N} \sum_{i=1}^N C_{\text{match}}(y_i, \hat{y}_{\sigma(i)}), \quad (3)$$

where $C_{\text{match}}(y_i, \hat{y}_{\sigma(i)})$ is a pair-wise matching cost between ground truth y_i and a prediction with index $\sigma(i)$. We detail the matching cost in (8).

Set guidance loss. By the permutation-invariant nature of the transformer, the prediction order cannot be determined. This raises a question: how can we match the predictions with corresponding queries? To answer the question, we introduce a set guidance loss that forces each prediction to associate with a specific sentence query. Given K input queries, N proposals are uniformly partitioned into K subsets. The proposals within the j th subset are trained to

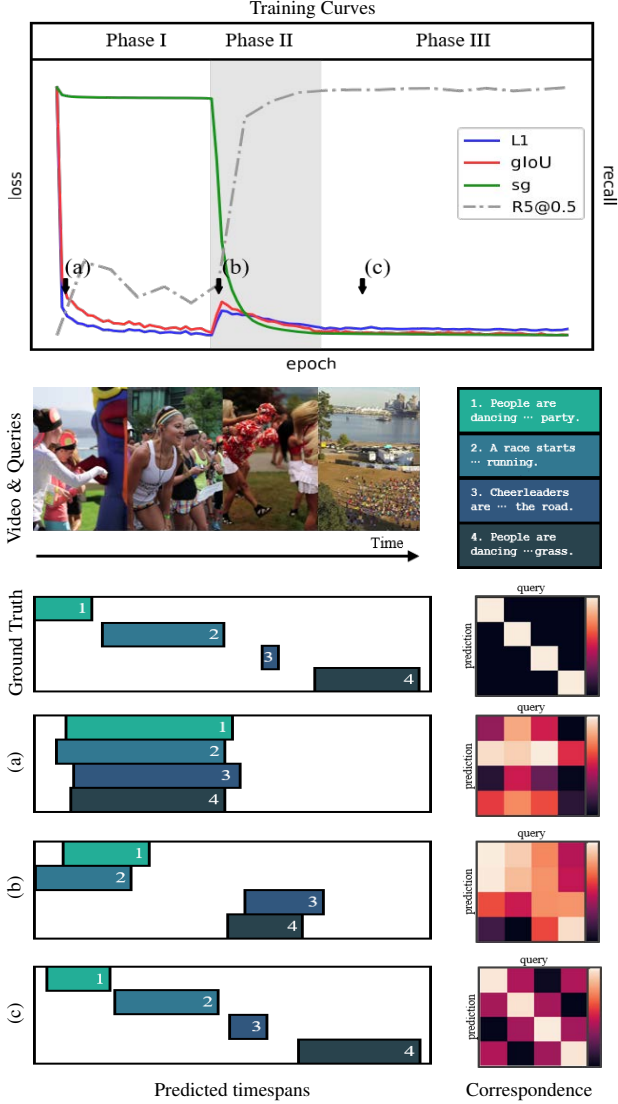


Figure 3. Visualization of timespan predictions (left) and prediction-query correspondences (right) at three different points in the training curves (top): (a) At early training, neither spans nor order is accurate. (b) During the search space **exploration**, the spans are in the process of aligning with the targets, but they are unordered. (c) After proposals **match** the corresponding targets, the predicted spans are accurately aligned with the paired targets.

predict the j th query by set guidance loss. Formally, we denote the probability that the prediction corresponds to the target query q_i (i.e., softmaxed correspondence) as $\hat{p}_{\sigma(i)}(q_i)$ for the prediction with index $\sigma(i)$. The set guidance loss is simply defined as a negative log-likelihood loss:

$$\mathcal{L}_{sg}(q_i) = - \sum_i \log \hat{p}_{\sigma(i)}(q_i). \quad (4)$$

While all proposals collaboratively predict a set of timespans via parallel decoding, the set guidance loss leads proposals to predict target-specific timespans.

Span localization loss. Our span localization loss is a linear combination of the ℓ_1 loss and the generalized IoU (gIoU) loss [35]:

$$\mathcal{L}_{span}(t_i, \hat{t}_{\sigma(i)}) = \lambda_{L1} \mathcal{L}_{L1}(t_i, \hat{t}_{\sigma(i)}) + \lambda_{iou} \mathcal{L}_{iou}(t_i, \hat{t}_{\sigma(i)}), \quad (5)$$

where $\hat{t}_{\sigma(i)}$ is the predicted timespan for the prediction with index $\sigma(i)$, and $\lambda_{L1}, \lambda_{iou} \in \mathbb{R}$ are balancing hyperparameters. While two loss terms share the same objective, they have subtle differences. The ℓ_1 loss will have different scales for short and long timespans, even if relative errors are similar, whereas gIoU loss is robust to varying scales.

$$\mathcal{L}_{L1}(t_i, \hat{t}_{\sigma(i)}) = \|t_i^s - \hat{t}_{\sigma(i)}^s\|_1 + \|t_i^e - \hat{t}_{\sigma(i)}^e\|_1, \quad (6)$$

$$\mathcal{L}_{iou}(t_i, \hat{t}_{\sigma(i)}) = 1 - \left(\frac{|t_i \cap \hat{t}_{\sigma(i)}|}{|t_i \cup \hat{t}_{\sigma(i)}|} - \frac{|T(t_i, \hat{t}_{\sigma(i)}) \setminus t_i \cup \hat{t}_{\sigma(i)}|}{|T(t_i, \hat{t}_{\sigma(i)})|} \right). \quad (7)$$

$|\cdot|$ means temporal area and \setminus means set subtraction. \cup and \cap are used for union and intersection of timespans. $T(t_i, \hat{t}_{\sigma(i)})$ is a tight bound of span containing t_i and $\hat{t}_{\sigma(i)}$.

Final set prediction loss. Both the target query prediction and timespan prediction are factored into the matching cost. We define matching cost using these notations:

$$\mathcal{C}_{match}(y_i, \hat{y}_{\sigma(i)}) = - \mathbb{1}_{\{q_i \neq \emptyset\}} \hat{p}_{\sigma(i)}(q_i) + \mathbb{1}_{\{q_i \neq \emptyset\}} \mathcal{L}_{span}(t_i, \hat{t}_{\sigma(i)}), \quad (8)$$

where $\mathbb{1}$ indicates the indicator function. Here, we consider the K matched predictions as positives (i.e., $q_i \neq \emptyset$), and the remaining $(N - K)$ predictions as negatives (i.e., $q_i = \emptyset$). Contrary to the loss, we do not use the negative log likelihood for the set guidance loss, but rather approximate it to $1 - p_{\sigma(i)}(q_i)$. We omit a constant 1 since it does not change the matching. Based on the matching results, our final set prediction loss is defined as:

$$\mathcal{L}_{set}(y, \hat{y}) = \sum_{i=1}^N [\lambda_{sg} \mathcal{L}_{sg}(q_i) + \mathbb{1}_{\{q_i \neq \emptyset\}} \mathcal{L}_{span}(t_i, \hat{t}_{\sigma(i)})], \quad (9)$$

where λ_{sg} is a loss coefficient. Only the positives are optimized to predict the corresponding ground truth timespans.

Unifying two streams of methods. Our approach inherits only the advantages from the *proposal-based* and the *proposal-free* methods. We use the proposals, the core concept of the *proposal-based* methods, to encourage positive proposals to have higher similarities and suppress the negative proposals to have lower similarities with ground truth. However, since *proposal-based* methods view video grounding as a classification problem, their performances are largely limited by hand-crafted components, such as predefined anchors and windows. Our approach differs from the *proposal-based* methods in that it incorporates the flexibility of *proposal-free* methods. We make every proposal learnable, allowing them to be fine-tuned within the

training pipeline and dynamically transformed into more reliable proposals without the need for heuristics.

In order to put two complementary properties into a single model, we employ two losses: set guidance loss and span localization loss. The combination of all training schemes condenses into a new video grounding paradigm named explore-and-match. As shown in Fig. 3, the set guidance loss and the span localization loss tend to show different patterns in training curves, where the former generates a cliff-like loss curve and the latter degrades smoothly. At the beginning of the training (Phase I: Fig. 3(a)), predicted timespans are almost a random initialization without order. Before the sharp drop of a set guidance loss (Phase II: Fig. 3(b)), a set of timespans aligns with a set of ground truths in a target-agnostic manner. Interestingly, as the set guidance loss decreases, the ℓ_1 loss and gIoU loss rebound slightly to reorganize predictions to be target-specific. When all losses converge (Phase III: Fig. 3(c)), timespans become accurate to match the target query. We empirically found that our method leads proposals to explore the search space, and then try to accurately match the target. We note that the whole process is carried out in a systematic and holistic manner.

4. Experiments

We first describe our experimental settings. Next, we report our main results on two challenging benchmarks: *ActivityCaptions* and *Charades-STA*. Lastly, we provide detailed ablation studies on the model variants and losses, and analyze how VIDGTR works with visualizations.²

4.1. Experimental Setup

Datasets. 1) *ActivityCaptions* [3, 20] contains about 20K untrimmed videos with language descriptions and temporal annotations, which was originally developed for the task of dense video captioning [20]. Following the convention, we use val_1 for validation and val_2 for testing since the test annotations are not publicly released. We also follow the standard split [52]. 2) *Charades-STA* [13] is built on Charades [38] and contains 6,672 videos of daily indoors activities. Each video is about 30 seconds long on average. We employ 12,408 video-sentence pairs for train and 3,720 pairs for test, as in previous studies.

Evaluation metrics. Following [29, 52], we adopt two standard evaluation metrics for video grounding: 1) “ $R_\alpha@ \mu$ ”, which denotes the percentage of test samples that have at least one correct result in top- α retrieved results, *i.e.*, Recall. Here, the correct results indicate that IoU with ground truth is larger than threshold μ . 2) “mIoU”, which averages the IoU between predictions and ground truths over all testing samples to compare the overall performance.

²We provide additional experiments in the supplementary material.

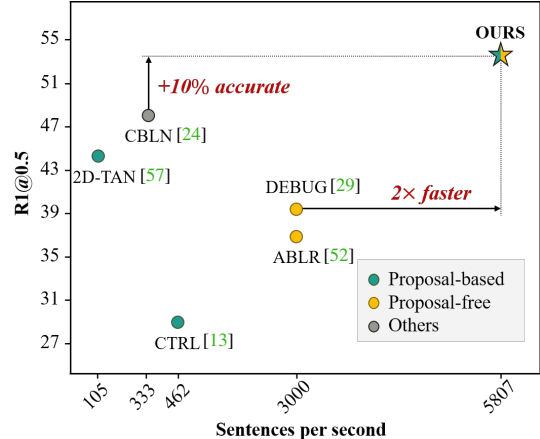


Figure 4. VIDGTR achieves **10% of performance gain** for R1@0.5 metric while being **2× faster** than previous baselines on *ActivityCaptions* dataset. The average inference speed is measured by the number of localized sentences per second.

Technical details. We train VIDGTR using AdamW [28] with an initial learning rate of $1e-4$ and weight decay of $1e-4$ for a batch size of 16. We use a linear learning rate decay by a factor of 10. We consider Xavier initialization [16] to set the initial values of all transformer weights. We use 64 frames that are uniformly sampled from video with four sentences as an input. We resize every frame to 112×112 . The number of learnable proposals is proportionally set to 10 times the number of input queries. For a fair evaluation with baselines, we extract video representations with C3D [40] pretrained on Sports-1M [19], and for the language part, we initialize each word with GloVe embeddings [32] and obtain sentence representation via 2-layer bi-LSTM [18]. In training, we set our overall loss weight $\lambda_{L1} : \lambda_{IoU} : \lambda_{sg}$ to 1 : 3 : 2. We also use an auxiliary decoding loss [1] in decoder layers to speed up the convergence. The initial proposals are filled with learnable weights [4].

4.2. Main Results

Comparison with state-of-the-art approaches. We compare VIDGTR against recently proposed video grounding methods, which can be largely categorized into three groups: 1) *proposal-based*: CTRL [13], TGN [5], 2D-TAN [57], CSMGAN [25], MSA [56], 2) *proposal-free*: ABLR [52], DEBUG [29], DRN [53], VSLNET [55], CP-NET [22], and 3) *etc*: BPNet [47], CBLN [24]. VIDGTR with C3D backbone, named VIDGTR-C3D, sets new state-of-the-arts on two benchmarks (see Table 1): *ActivityCaptions* [3, 20] and *Charades-STA* [13]. Especially for R1@0.5 metric on *ActivityCaptions* dataset, VIDGTR-C3D achieved about 10% performance gain compared to CBLN [24]. We further improve the performance of VIDGTR by using CLIP [34] as a backbone, *i.e.*, VIDGTR-CLIP, where a massive amount of image-text pairs are pre-trained with contrastive learning. Even freezing the back-

ActivityCaption						
Methods		R1@0.5	R1@0.7	R5@0.5	R5@0.7	mIoU
PB	TGN [5]	27.93	-	44.20	-	-
	2D-TAN [57]	44.51	26.54	77.13	61.96	-
	CSMGAN [25]	49.11	29.15	77.43	59.63	-
	MSA [56]	48.02	31.78	78.02	63.18	-
PF	ABLR [52]	36.79	-	-	-	36.99
	DEBUG [29]	39.72	-	-	-	39.51
	DRN [53]	45.45	24.36	77.97	50.30	-
	VSLNET [55]	43.22	26.16	-	-	43.19
	CPNET [22]	40.65	21.63	-	-	40.65
etc	BPNET [47]	42.07	24.69	-	-	42.11
	CBLN [24]	48.12	27.60	79.32	63.41	-
VidGTR-C3D						
		53.27	27.93	78.19	57.82	51.00
VidGTR-CLIP		58.79	33.38	77.47	59.68	54.29

Charades-STA						
Methods		R1@0.5	R1@0.7	R5@0.5	R5@0.7	mIoU
PB	CTRL [13]	23.63	8.89	58.92	29.52	-
	2D-TAN [57]	39.70	27.1	80.32	51.26	-
PF	DEBUG [29]	37.39	17.69	-	-	36.34
	DRN [53]	45.40	26.40	88.01	55.38	-
	VSLNET [55]	47.31	30.19	-	-	45.15
	CPNET [22]	40.32	22.47	-	-	37.36
etc	BPNET [47]	38.25	20.51	-	-	38.03
	CBLN [24]	47.94	28.22	88.20	57.47	-
VidGTR-C3D						
		46.74	22.72	84.67	52.01	42.00
VidGTR-CLIP		48.60	25.21	87.79	52.18	45.01

Table 1. **Comparison with the state-of-the-arts** on two benchmark datasets: *ActivityCaption* and *Charades-STA*. PB and PF denote *proposal-based* and *proposal-free* approaches, respectively.

bone in the training phase, we observed that CLIP significantly boosts the performance, implying that visual-linguistic domain alignment is important.

Inference speed. We compare several methods in terms of inference speed required to localize a single sentence query in Fig. 4. Our VIDGTR takes an average of 10ms to process a language query on *ActivityCaptions* dataset. VIDGTR runs much faster than the previous video grounding methods, especially $2\times$ faster than DEBUG [29]. Furthermore, our set matching formulation eliminates the time-consuming pre- or post-processing stage, such as dense proposal generation and non-maximum suppression.

4.3. Analysis

Loss ablations. We analyze the impact of the loss terms in Table 2: ℓ_1 loss (\mathcal{L}_{L1}), gIoU loss (\mathcal{L}_{iou}), and set guidance loss (\mathcal{L}_{sg}). Since identifying the target query is essential, we always use set guidance loss for all cases. When both L1 and gIoU are turned off, the predictions collapse into a single timespan; thus R1@0.5 and R5@0.5 show al-

\mathcal{L}_{sg}	\mathcal{L}_{L1}	\mathcal{L}_{iou}	R1@0.5	R1@0.7	R5@0.5	R5@0.7	mIoU
✓			24.30	9.60	24.69	9.75	26.9
✓	✓		41.42	18.25	72.55	54.90	41.25
✓		✓	50.15	27.90	72.32	55.50	48.01
✓	✓	✓	58.79	33.38	77.47	59.68	53.00

Table 2. **Ablation results of the loss functions.**

Methods	R1@0.5	R1@0.7	R5@0.5	R5@0.7	mIoU
Sim	13.11	2.75	13.15	2.79	23.73
Att	34.36	18.10	82.42	63.31	39.16
Cos	58.79	33.38	77.47	59.68	53.00

Table 3. **Choices for pred-query correspondence measure.**

most the same results. When either L1 or gIoU losses is disabled, performance suffers significantly, implying that they are both required for accurate timespan localization. As using all three losses yields the best result, we confirm that two sub losses of span localization loss (L1 and gIoU) operate complementarily with absolute or relative criteria for timespan prediction.

Correspondence measures. We compare the various measures to calculate the correspondence between prediction and query in Table 3, which is then used in set guidance loss. In practice, we consider proposal-target matching using decoder output and textual part of encoder output. The encoder-decoder attention weight (Att) is an intuitive way to determine which part of the encoder output each proposal corresponds to. Since it has direct access to the global context, it performs well especially for the R5 metric, but falls short for the rigorous R1 metric. We see that using cosine similarity (Cos) dramatically improves performance than directly applying dot product similarity (Sim), meaning that removing the size constraint eases optimization.

Model size. To examine the effect of model size, we vary the number of transformer encoder-decoder layers (see Table 4). We first compare the two asymmetric structures (#Enc-#Dec): 2-1 vs. 1-2. Compared to the former, the latter falls 2.18 points in R5@0.5 and 6.33 points in R5@0.7 metrics, showing that the contextualization in encoder is important in generating high-quality proposals. As the size of the transformer increases, the R1 metric gradually improves, while R5 does not change appreciably. This suggests that increasing the size of the transformer has the effect of focusing on selecting better prediction among the candidates. However, considering that the performance degrades in 6-6, stacking more encoder-decoders does not always guarantee higher performance. Among several variants, we found that 4-4 shows the optimal performance.

Number of learnable proposals. We search for the optimal number of proposals per language query in Table 5. A

#Enc	#Dec	R1@0.5	R1@0.7	R5@0.5	R5@0.7	mIoU
1	1	48.16	25.55	79.38	64.34	48.02
2	1	48.20	26.08	77.57	64.05	47.67
1	2	48.30	25.40	75.39	57.72	47.97
2	2	55.22	31.13	76.39	61.65	50.99
3	3	53.32	26.62	74.65	58.44	48.92
4	4	58.79	33.38	77.47	59.68	53.00
5	5	56.11	33.82	79.15	60.70	52.04
6	6	46.75	21.41	77.74	63.45	46.34

Table 4. Model variants w.r.t Encoder-Decoder size.

#Proposals	R1@0.5	R1@0.7	R5@0.5	R5@0.7	mIoU
5	48.74	25.40	86.37	70.68	48.03
10	58.79	33.38	77.47	59.68	53.00
15	34.26	16.17	65.59	47.35	39.74
20	6.64	2.16	18.02	6.11	13.07

Table 5. Effect of the number of learnable proposals per query.

small number of proposals limits sufficient interactions between positives and negatives, resulting in sub-optimal performance, whereas an excessive quantity of proposals reduces accuracy by generating too many negatives. There is a trade-off between R5 and mIoU metrics around the appropriate number of proposals. Between them, having 10 learnable proposals per query yielded the best results.

Qualitative examples. In Fig. 9, we show a sample video grounding result, where the bars lie along the time axis represent the timespans grounded on the query. The predictions (color bar) generated by VIDGTR align with the target timespans (empty bar). As seen in the proposal-video attention map, we observe that the areas that learnable proposals mostly attend to are roughly divided by the number of queries; for example, the third prediction focuses on the end of the video. This means that proposals within the same subset consider similar parts of the video contexts in order to predict the target query.³

Distribution of learnable proposals. We visualize the timespan predictions of learnable proposals in Fig. 6. We observe that 10 out of all learnable proposals in the VIDGTR decoder mostly showed different patterns, which implies that VIDGTR learns different specializations for each proposal. More specifically, each proposal has several operating modes attending to different time zones and durations. For example, the top third proposal learns about a long period of time at the beginning of the videos. Overall, all proposals have a mode that predicts video-wide durations, which is colored in blue.

³More qualitative results are presented in the supplementary material.

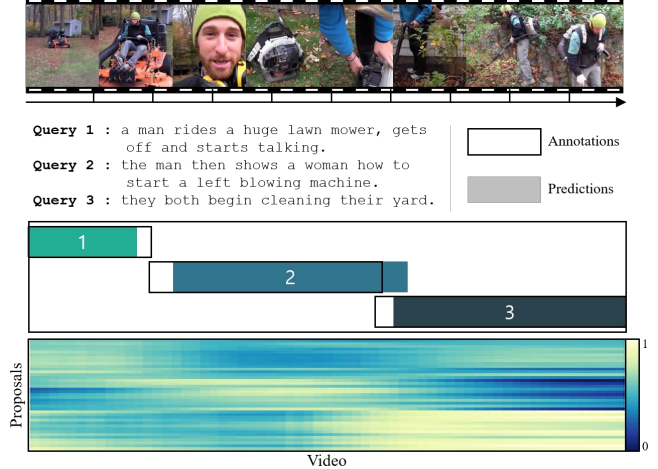


Figure 5. Video grounding results with proposal-video attention map. Note that each subset of learnable proposals in the VIDGTR decoder attends to the corresponding video contexts to predict the target timespans. The color indicates the attention.

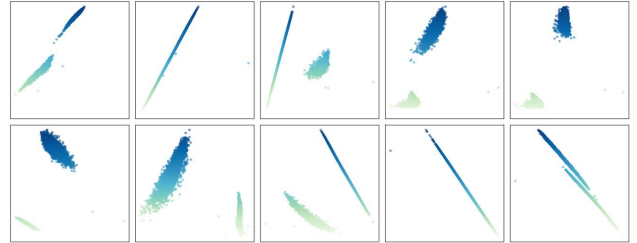


Figure 6. Visualization of timespan predictions on all video-query pairs from ActivityCaptions, for 10 out of all learnable proposals. Each prediction is represented by a colored point on the horizontal (center) and vertical (width) axes, where the color indicates the width. We observe that each learnable proposal learns to specialize on certain time zones and durations.

5. Conclusion

In this study, we introduced explore-and-match, a new video grounding paradigm that unifies *proposal-based* and *proposal-free* approaches; our approach inherits the former concept while proposals are flexible as in the latter. We view video grounding as a direct set prediction problem. An end-to-end trainable VIDGTR is designed to solve this problem on top of transformer encoder-decoder architecture. VIDGTR predicts timespans in parallel, which are grounded on abundant video-text contexts. We employ bipartite matching in tandem with two key losses: 1) set guidance loss, which forces to match the target, and 2) span localization loss, which regress each proposal to fit the timespan. Our approach diversifies proposals in the explore step and matches each proposal to specific sentence in the match step. VIDGTR achieves new state-of-the-art results on two challenging benchmarks while doubling the inference speed. We hope our exploration and findings facilitate future research on video grounding.

References

- [1] Rami Al-Rfou, Dokook Choe, Noah Constant, Mandy Guo, and Llion Jones. Character-Level Language Modeling With Deeper Self-Attention. In *AAAI*, volume 33, pages 3159–3166, 2019. 6
- [2] Lisa Anne Hendricks, Oliver Wang, Eli Shechtman, Josef Sivic, Trevor Darrell, and Bryan Russell. Localizing Moments in Video With Natural Language. In *ICCV*, pages 5803–5812, 2017. 1, 2
- [3] Fabian Caba Heilbron, Victor Escorcia, Bernard Ghanem, and Juan Carlos Niebles. Activitynet: A Large-Scale Video Benchmark for Human Activity Understanding. In *CVPR*, pages 961–970, 2015. 2, 6
- [4] Nicolas Carion, Francisco Massa, Gabriel Synnaeve, Nicolas Usunier, Alexander Kirillov, and Sergey Zagoruyko. End-to-End Object Detection With Transformers. In *ECCV*, pages 213–229. Springer, 2020. 3, 6
- [5] Jingyuan Chen, Xinpeng Chen, Lin Ma, Zequn Jie, and Tat-Seng Chua. Temporally Grounding Natural Sentence in Video. In *EMNLP*, pages 162–171, 2018. 1, 2, 6, 7
- [6] Long Chen, Chujie Lu, Siliang Tang, Jun Xiao, Dong Zhang, Charlie Tan, and Xiaolin Li. Rethinking the Bottom-Up Framework for Query-Based Video Localization. In *AAAI*, volume 34, pages 10551–10558, 2020. 1, 2
- [7] Shaoxiang Chen, Wenhao Jiang, Wei Liu, and Yu-Gang Jiang. Learning Modality Interaction for Temporal Sentence Localization and Event Captioning in Videos. In *ECCV*, pages 333–351. Springer, 2020. 1, 2
- [8] Shaoxiang Chen and Yu-Gang Jiang. Hierarchical Visual-Textual Graph for Temporal Activity Localization via Language. In *ECCV*, pages 601–618. Springer, 2020. 1, 2
- [9] Shizhe Chen, Yida Zhao, Qin Jin, and Qi Wu. Fine-Grained Video-Text Retrieval With Hierarchical Graph Reasoning. In *CVPR*, pages 10638–10647, 2020. 1
- [10] Zhenfang Chen, Lin Ma, Wenhan Luo, Peng Tang, and Kwan-Yee K Wong. Look Closer To Ground Better: Weakly-Supervised Temporal Grounding of Sentence in Video. *arXiv preprint arXiv:2001.09308*, 2020. 1
- [11] Alexey Dosovitskiy, Lucas Beyer, Alexander Kolesnikov, Dirk Weissenborn, Xiaohua Zhai, Thomas Unterthiner, Mostafa Dehghani, Matthias Minderer, Georg Heigold, Sylvain Gelly, et al. An Image Is Worth 16x16 Words: Transformers for Image Recognition at Scale. *arXiv preprint arXiv:2010.11929*, 2020. 4
- [12] Valentin Gabeur, Chen Sun, Karteek Alahari, and Cordelia Schmid. Multi-Modal Transformer for Video Retrieval. In *ECCV*, pages 214–229. Springer, 2020. 1
- [13] Jiyang Gao, Chen Sun, Zhenheng Yang, and Ram Nevatia. TALL: Temporal Activity Localization via Language Query. In *ICCV*, pages 5267–5275, 2017. 1, 2, 6, 7
- [14] Runzhou Ge, Jiyang Gao, Kan Chen, and Ram Nevatia. Mac: Mining Activity Concepts for Language-Based Temporal Localization. In *WACV*, pages 245–253. IEEE, 2019. 1, 2
- [15] Soham Ghosh, Anuva Agarwal, Zarana Parekh, and Alexander Hauptmann. Excl: Extractive Clip Localization Using Natural Language Descriptions. *arXiv preprint arXiv:1904.02755*, 2019. 1, 2
- [16] Xavier Glorot and Yoshua Bengio. Understanding the Difficulty of Training Deep Feedforward Neural Networks. In *AISTATS*, pages 249–256. JMLR Workshop and Conference Proceedings, 2010. 6
- [17] Lisa Anne Hendricks, Oliver Wang, Eli Shechtman, Josef Sivic, Trevor Darrell, and Bryan Russell. Localizing Moments in Video With Temporal Language. *arXiv preprint arXiv:1809.01337*, 2018. 1, 2
- [18] Sepp Hochreiter and Jürgen Schmidhuber. Long Short-Term Memory. *Neural computation*, 9(8):1735–1780, 1997. 3, 6
- [19] Andrej Karpathy, George Toderici, Sanketh Shetty, Thomas Leung, Rahul Sukthankar, and Li Fei-Fei. Large-Scale Video Classification With Convolutional Neural Networks. In *CVPR*, pages 1725–1732, 2014. 6
- [20] Ranjay Krishna, Kenji Hata, Frederic Ren, Li Fei-Fei, and Juan Carlos Niebles. Dense-Captioning Events in Videos. In *ICCV*, pages 706–715, 2017. 2, 6
- [21] Harold W Kuhn. The Hungarian Method for the Assignment Problem. *Naval research logistics quarterly*, 2(1-2):83–97, 1955. 2, 3, 4
- [22] Kun Li, Dan Guo, and Meng Wang. Proposal-Free Video Grounding with Contextual Pyramid Network. In *AAAI*, volume 35, pages 1902–1910, 2021. 6, 7
- [23] Kevin Lin, Lijuan Wang, and Zicheng Liu. End-to-End Human Pose and Mesh Reconstruction With Transformers. In *CVPR*, pages 1954–1963, 2021. 3
- [24] Daizong Liu, Xiaoye Qu, Jianfeng Dong, Pan Zhou, Yu Cheng, Wei Wei, Zichuan Xu, and Yulai Xie. Context-aware Biaffine Localizing Network for Temporal Sentence Grounding. In *CVPR*, pages 11235–11244, 2021. 6, 7
- [25] Daizong Liu, Xiaoye Qu, Xiao-Yang Liu, Jianfeng Dong, Pan Zhou, and Zichuan Xu. Jointly Cross-And Self-Modal Graph Attention Network for Query-Based Moment Localization. In *ACMMM*, pages 4070–4078, 2020. 1, 2, 6, 7
- [26] Meng Liu, Xiang Wang, Liqiang Nie, Qi Tian, Baoquan Chen, and Tat-Seng Chua. Cross-Modal Moment Localization in Videos. In *ACMMM*, pages 843–851, 2018. 1, 2
- [27] Ruijin Liu, Zejian Yuan, Tie Liu, and Zhiliang Xiong. End-to-End Lane Shape Prediction With Transformers. In *WACV*, pages 3694–3702, 2021. 3
- [28] Ilya Loshchilov and Frank Hutter. Decoupled Weight Decay Regularization. *arXiv preprint arXiv:1711.05101*, 2017. 6
- [29] Chujie Lu, Long Chen, Charlie Tan, Xiaolin Li, and Jun Xiao. DEBUG: A Dense Bottom-Up Grounding Approach for Natural Language Video Localization. In *EMNLP-IJCNLP*, pages 5144–5153, 2019. 1, 2, 6, 7
- [30] Antoine Miech, Dimitri Zhukov, Jean-Baptiste Alayrac, Makarand Tapaswi, Ivan Laptev, and Josef Sivic. Howto100m: Learning a Text-Video Embedding by Watching Hundred Million Narrated Video Clips. In *ICCV*, pages 2630–2640, 2019. 1
- [31] Jonghwan Mun, Minsu Cho, and Bohyung Han. Local-Global Video-Text Interactions for Temporal Grounding. In *CVPR*, pages 10810–10819, 2020. 1, 2
- [32] Jeffrey Pennington, Richard Socher, and Christopher D Manning. Glove: Global Vectors for Word Representation. In *EMNLP*, pages 1532–1543, 2014. 3, 6
- [33] Xiaoye Qu, Pengwei Tang, Zhikang Zou, Yu Cheng, Jianfeng Dong, Pan Zhou, and Zichuan Xu. Fine-Grained Iterative Attention Network for Temporal Language Localization

- in Videos. In *ACMMM*, pages 4280–4288, 2020. 1, 2
- [34] Alec Radford, Jong Wook Kim, Chris Hallacy, Aditya Ramesh, Gabriel Goh, Sandhini Agarwal, Girish Sastry, Amanda Askell, Pamela Mishkin, Jack Clark, et al. Learning Transferable Visual Models From Natural Language Supervision. *arXiv preprint arXiv:2103.00020*, 2021. 4, 6
- [35] Hamid Rezaatofighi, Nathan Tsoi, JunYoung Gwak, Amir Sadeghian, Ian Reid, and Silvio Savarese. Generalized Intersection Over Union: A Metric and a Loss for Bounding Box Regression. In *CVPR*, pages 658–666, 2019. 5
- [36] Cristian Rodriguez, Edison Marrese-Taylor, Fatemeh Sadat Saleh, Hongdong Li, and Stephen Gould. Proposal-Free Temporal Moment Localization of a Natural-Language Query in Video Using Guided Attention. In *WACV*, pages 2464–2473, 2020. 1, 2
- [37] Zheng Shou, Dongang Wang, and Shih-Fu Chang. Temporal Action Localization in Untrimmed Videos via Multi-Stage CNNs. In *CVPR*, pages 1049–1058, 2016. 2
- [38] Gunnar A Sigurdsson, Gül Varol, Xiaolong Wang, Ali Farhadi, Ivan Laptev, and Abhinav Gupta. Hollywood in Homes: Crowdsourcing Data Collection for Activity Understanding. In *ECCV*, pages 510–526. Springer, 2016. 6
- [39] Mattia Soldan, Mengmeng Xu, Sisi Qu, Jesper Tegner, and Bernard Ghanem. VLG-Net: Video-Language Graph Matching Network for Video Grounding. In *ICCV*, pages 3224–3234, 2021. 1
- [40] Du Tran, Lubomir Bourdev, Rob Fergus, Lorenzo Torresani, and Manohar Paluri. Learning Spatiotemporal Features With 3D Convolutional Networks. In *ICCV*, pages 4489–4497, 2015. 3, 6
- [41] Ashish Vaswani, Noam Shazeer, Niki Parmar, Jakob Uszkoreit, Llion Jones, Aidan N Gomez, Łukasz Kaiser, and Illia Polosukhin. Attention is All You Need. In *NeurIPS*, pages 5998–6008, 2017. 2, 3
- [42] Hao Wang, Zheng-Jun Zha, Xuejin Chen, Zhiwei Xiong, and Jiebo Luo. Dual Path Interaction Network for Video Moment Localization. In *ACMMM*, pages 4116–4124, 2020. 1, 2
- [43] Hao Wang, Zheng-Jun Zha, Liang Li, Dong Liu, and Jiebo Luo. Structured Multi-Level Interaction Network for Video Moment Localization via Language Query. In *CVPR*, pages 7026–7035, 2021. 1, 2
- [44] Huiyu Wang, Yukun Zhu, Hartwig Adam, Alan Yuille, and Liang-Chieh Chen. Max-DeepLab: End-to-End Panoptic Segmentation With Mask Transformers. In *CVPR*, pages 5463–5474, 2021. 3
- [45] Jingwen Wang, Lin Ma, and Wenhao Jiang. Temporally Grounding Language Queries in Videos by Contextual Boundary-Aware Prediction. In *AAAI*, volume 34, pages 12168–12175, 2020. 1, 2
- [46] Yuqing Wang, Zhaoliang Xu, Xinlong Wang, Chunhua Shen, Baoshan Cheng, Hao Shen, and Huaxia Xia. End-to-End Video Instance Segmentation With Transformers. In *CVPR*, pages 8741–8750, 2021. 3
- [47] Shaoning Xiao, Long Chen, Songyang Zhang, Wei Ji, Jian Shao, Lu Ye, and Jun Xiao. Boundary Proposal Network for Two-Stage Natural Language Video Localization. In *AAAI*, volume 35, pages 2986–2994, 2021. 1, 6, 7
- [48] Huijuan Xu, Kun He, Bryan A Plummer, Leonid Sigal, Stan Sclaroff, and Kate Saenko. Multilevel Language and Vision Integration for Text-To-Clip Retrieval. In *AAAI*, volume 33, pages 9062–9069, 2019. 1, 2
- [49] Xun Yang, Jianfeng Dong, Yixin Cao, Xun Wang, Meng Wang, and Tat-Seng Chua. Tree-Augmented Cross-Modal Encoding for Complex-Query Video Retrieval. In *SIGIR*, pages 1339–1348, 2020. 1
- [50] Yitian Yuan, Lin Ma, Jingwen Wang, Wei Liu, and Wenwu Zhu. Semantic Conditioned Dynamic Modulation for Temporal Sentence Grounding in Videos. *arXiv preprint arXiv:1910.14303*, 2019. 1, 2
- [51] Yitian Yuan, Lin Ma, Jingwen Wang, Wei Liu, and Wenwu Zhu. Semantic Conditioned Dynamic Modulation for Temporal Sentence Grounding in Videos. *TPAMI*, 2020. 1
- [52] Yitian Yuan, Tao Mei, and Wenwu Zhu. To Find Where You Talk: Temporal Sentence Localization in Video With Attention Based Location Regression. In *AAAI*, volume 33, pages 9159–9166, 2019. 1, 2, 6, 7
- [53] Runhao Zeng, Haoming Xu, Wenbing Huang, Peihao Chen, Minghui Tan, and Chuang Gan. Dense Regression Network for Video Grounding. In *CVPR*, pages 10287–10296, 2020. 1, 2, 6, 7
- [54] Da Zhang, Xiyang Dai, Xin Wang, Yuan-Fang Wang, and Larry S Davis. Man: Moment Alignment Network for Natural Language Moment Retrieval via Iterative Graph Adjustment. In *CVPR*, pages 1247–1257, 2019. 1, 2
- [55] Hao Zhang, Aixin Sun, Wei Jing, and Joey Tianyi Zhou. Span-Based Localizing Network for Natural Language Video Localization. *arXiv preprint arXiv:2004.13931*, 2020. 1, 2, 6, 7
- [56] Mingxing Zhang, Yang Yang, Xinghan Chen, Yanli Ji, Xing Xu, Jingjing Li, and Heng Tao Shen. Multi-Stage Aggregated Transformer Network for Temporal Language Localization in Videos. In *CVPR*, pages 12669–12678, 2021. 1, 2, 6, 7
- [57] Songyang Zhang, Houwen Peng, Jianlong Fu, and Jiebo Luo. Learning 2d Temporal Adjacent Networks for Moment Localization With Natural Language. In *AAAI*, volume 34, pages 12870–12877, 2020. 1, 2, 6, 7
- [58] Zhu Zhang, Zhijie Lin, Zhou Zhao, and Zhenxin Xiao. Cross-Modal Interaction Networks for Query-Based Moment Retrieval in Videos. In *SIGIR*, pages 655–664, 2019. 1, 2
- [59] Cheng Zou, Bohan Wang, Yue Hu, Junqi Liu, Qian Wu, Yu Zhao, Boxun Li, Chenguang Zhang, Chi Zhang, Yichen Wei, et al. End-to-End Human Object Interaction Detection With HOI Transformer. In *CVPR*, pages 11825–11834, 2021. 3

A. Appendix

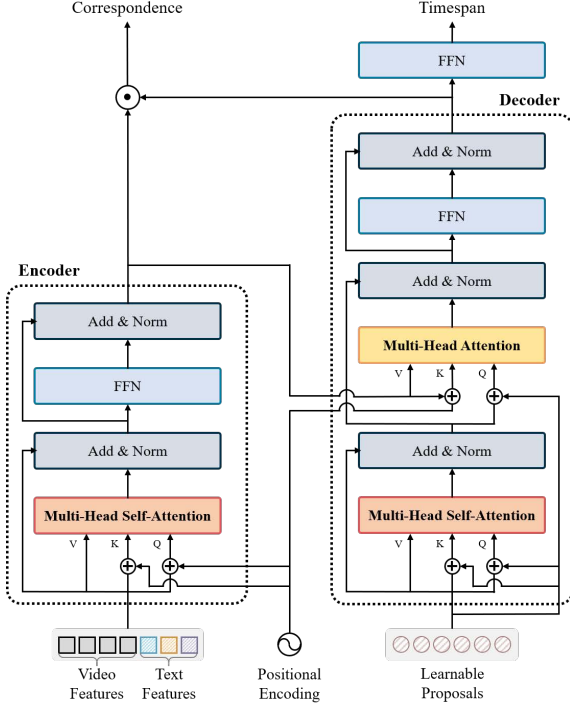


Figure 7. VIDGTR Architecture.

A.1. Architectural Details

We detail the architecture of VIDGTR in Fig. 7. The overall design is similar to that of original transformer encoder-decoder. First, the transformer encoder processes video-text features, which are extracted from the backbone, added with temporal positional encoding⁴ at each multi-head self-attention layer. Next, the decoder receives learnable proposals and encoder memory and process them with multiple multi-head self-attention and encoder-decoder attention layers. Finally, the output of decoder is used to generate the final set of predicted timespans, and also used to measure the correspondence between proposals and text queries.

A.2. Additional Experiments

Loss hyperparameters. We search for optimal loss hyperparameters in Table 6. We begin by setting the loss coefficients to 1:1:1 by default. While set guidance loss (λ_{sg}) is essential for query identity matching, the span localization loss (λ_{L1} and λ_{iou}) directly affects the accurate video grounding. This can be confirmed by varying the coefficient for each term to 2 one-by-one. Among the three variations, we found that gIoU loss (λ_{iou}) is the most important term

⁴We use a fixed absolute encoding to represent the temporal positions.

in the loss function. This is because the relative measure is more robust to varying spans shifted over various time distributions. While maintaining the gIoU loss to hold the major term, 1:3:2 yields the best results in our setting.

Input analysis. In order to examine the effect according to the number of input video frames and the number of input sentences, we varied the numbers in Table 7 and Table 8, respectively. As we expect more frames to bring more temporal knowledge, too few frames miss the exact moment when the event occurs, leading to decrease in performance. However, the results reveal that a large number of frames does not always guarantees better results. This implies that adding more frames cause a trade-off in the optimization while increasing the sequence length. We found that 64 produces the best results. Using multiple sentences as input queries allows us to take advantage of the temporal contexts between language queries. In the R1 metric, using 4 sentences as an input outperforms using 3 sentences, while using 3 sentences as an input shows better results in the R5 metric. This is due to the fact that the average number of existing sentences in training split of *ActivityCaptions* is 3.739. We adopt 4 sentences as an input since we require a more accurate model on a stricter metric.

Positional encodings. In Table 9, we ablate the positional encodings used by VIDGTR. First, we disable positional encoding for both video and text input. As expected, temporally unorganized input severely degrades performance. The positional encoding of each modality input is then removed in turn. When the video positional encodings are disabled, the model is no longer able to utilize temporally coordinated video contexts. In addition, the temporal clue provided by textual positional encoding is significant in textual input since it aids in organizing the order of events. We use both positional encodings since both positional encoding largely contributes to the performance. In order to align the video and text in a different time axis, we employ two separate positional encodings for each modality input.

Training with explore-and-match scheme. In Fig. 8, we investigate the behavior of VIDGTR during training under the explore-and-match scheme. Starting from random initialization, the predictions starts to create some variations. Since then, they have become a state that can be adapted to any timespan by slightly overlapping the boundaries of several ground truths, and then attempt to match only the span to some extent regardless of its identity. After matching the identity, we observe that the predictions try to accurately fit the corresponding span in a fine-grained manner. We argue that this systematic behavior is carried out by a carefully designed training regime.

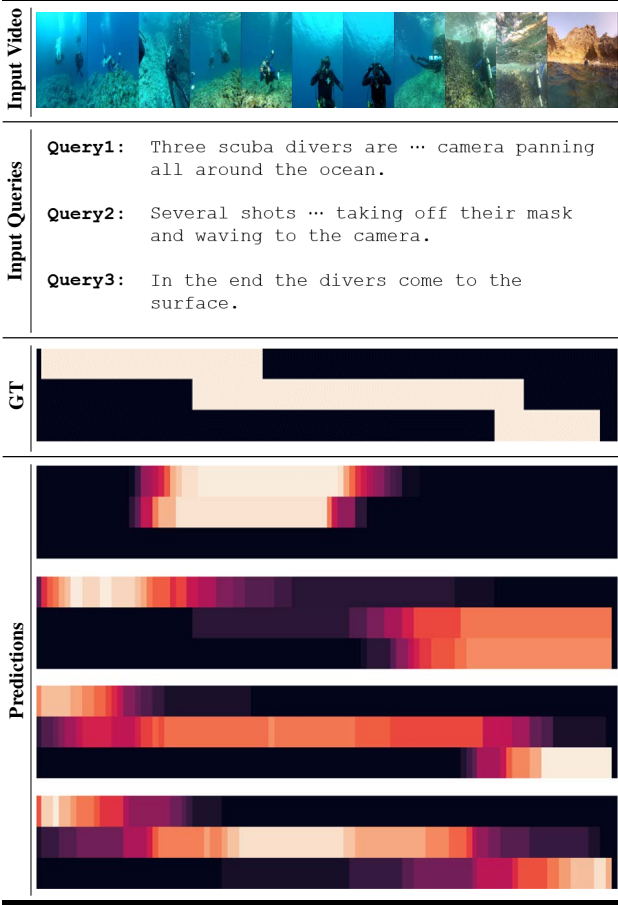


Figure 8. **Visualization of predictions throughout training under explore-and-match scheme.** Here, each row in predictions is represented in color — the brighter the color, the higher the probability of predictions — by overlapping the proposals that predict the corresponding query. The more overlapping the timespans predicted by the proposals, the brighter they become.

$\lambda_{L1}:\lambda_{iou}:\lambda_{sg}$	R1@0.5	R1@0.7	R5@0.5	R5@0.7	mIoU
1:1:1	53.39	30.79	80.68	60.76	51.24
2:1:1	56.42	31.59	78.90	63.03	52.77
1:2:1	58.03	31.23	78.02	60.49	52.15
1:1:2	57.41	32.91	77.09	57.49	53.50
1:3:1	49.59	28.03	66.81	48.78	48.18
1:3:2	58.79	33.38	77.47	59.68	53.00

Table 6. **Loss balancing parameters.**

A.3. More Qualitative Results

To better see how VIDGTR understands the video contexts, we provide additional qualitative examples and contrast the success and failure cases in Fig. 9. The results show that the VIDGTR successfully identifies the object described in the query and accurately localize the timespan, even if multiple objects appear in the video (row 1&2). Moreover, VIDGTR correctly reasons about the action that

#Frames	R1@0.5	R1@0.7	R5@0.5	R5@0.7	mIoU
16	47.93	23.34	72.30	51.31	42.53
32	52.15	28.77	74.01	55.13	50.46
64	58.79	33.38	77.47	59.68	53.00
128	53.73	29.55	77.42	60.77	51.11
256	48.35	24.39	73.36	54.23	47.89

Table 7. **Effect of the number of input frames.**

#Sentences	R1@0.5	R1@0.7	R5@0.5	R5@0.7	mIoU
2	33.86	17.31	70.41	44.00	38.73
3	46.15	22.03	81.58	63.17	47.05
4	58.79	33.38	77.47	59.68	53.00
5	35.41	17.51	69.19	48.74	39.58

Table 8. **Effect of the number of input sentences.**

Vid	Txt	R1@0.5	R1@0.7	R5@0.5	R5@0.7	mIoU
		25.71	12.69	66.34	41.45	29.85
✓		22.86	10.75	63.95	40.83	30.11
	✓	38.18	16.05	74.56	54.58	40.88
✓	✓	58.79	33.38	77.47	59.68	53.00

Table 9. **Positional Encodings.**

takes place from the first person point of view (row 3). Lastly, even if the same object appears repeatedly, VIDGTR distinguishes subtle contextual differences between them well (row 4). However, VIDGTR often fails to capture short-term events, especially when the object is too small (row 1&2). VIDGTR suffers when the time the event takes place is too long (e.g., whole video length) (row 3). Also, VIDGTR fails when the labeled timespan and the actual timespan where the query description matches the video content are significantly different (row 4).

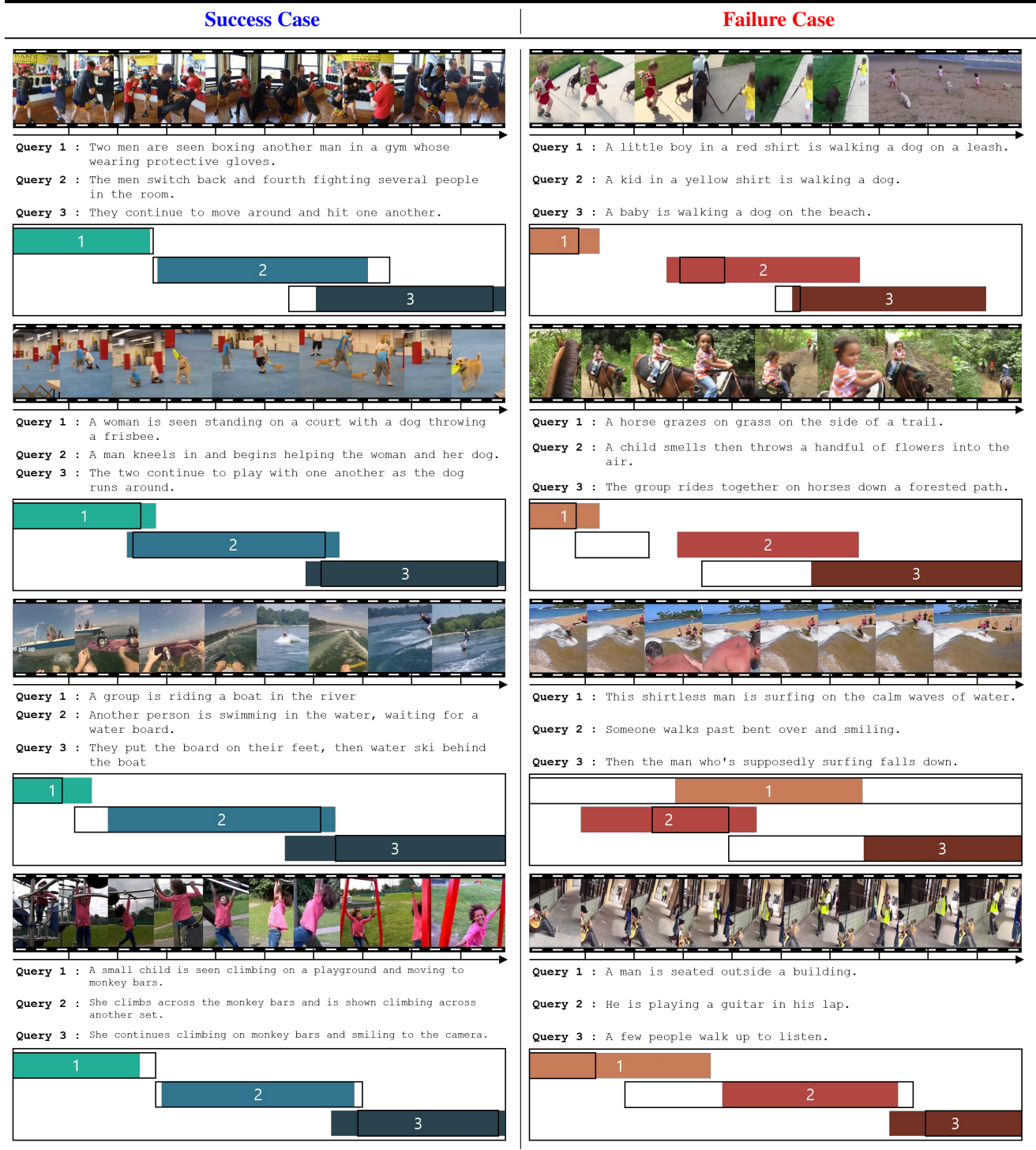


Figure 9. **Qualitative examples of success and failure cases** of VIDGTR on the *ActivityCaptions* dataset. The predicted timespan is considered correct only if it has sufficiently high IoU (*i.e.*, $\text{IoU} > 0.5$) with ground truth timespan. Empty bars represent ground truths, and colored bars represent predictions.